J. Geomag. Geoelectr., **25**, 39-62, 1973

An Array Study of Daily Magnetic Variations in Southeast Australia

D.J. BENNETT* and F.E.M. LILLEY

Department of Geophysics and Geochemistry, Australian National University, Canberra, A.C.T., Australia

(Received July 17, 1972; Revised December 22, 1972)

Three days of quiet diurnal magnetic variation have been analysed as recorded by an array of three-component variometers sited stretching inland from the coasts of Southeast Australia. Particular attention has been paid to the anomalous variations in the vertical component of magnetic field: before this can be studied properly a regional normal vertical field must be estimated and subtracted vectorially from that which is observed. A possible correlation between anomalous and normal vertical variations may indicate large scale induction in the oceans by the vertical variation field, as described by Bullard and Parker. However, comparison with estimates based on the calculations of Richards suggests that, whilst this inductive mechanism may give suitable values at the basic diurnal frequency, it does not appear to account for the coast effect observed at the second and third diurnal harmonics. The misfit of theory and observation is especially marked in the phase values. By contrast, the amplitudes and phases of the anomalous vertical variations of the first four diurnal harmonics all appear consistent with them being caused by the horizontal variation component at right angles to the coast line. If this is so it would require an electrical conductivity contrast between ocean and continent extending to depths sufficient to affect variations of 24-hour period.

1. Introduction

The analysis of naturally occurring variations of the earth's magnetic field is a well-established technique for examining the electrical conductivity structure of the earth. Global separations of variations of period one day or greater into parts of internal and external origin have been used to obtain models of the radial conductivity structure of the earth to great depths. Typically such studies suggest a sharp rise of electrical conductivity at a depth of a few hundred kilometres. The most recent studies of BANKS (1969) and PARKER (1970) suggest a rise of conductivity by one to two orders of magnitude to about 0.7 $(\text{ohm}\cdot\text{m})^{-1}$ at a depth greater than 400 km.

Many modern geophysical studies have however revealed that the earth's upper mantle shows marked non-radial variations of physical properties, a fact

* Present address: Institute for Geological Sciences, University of Texas at Dallas, U.S.A.

usually disregarded in such global magnetic variation analyses, which of necessity assume radial symmetry; and in recent years many studies of magnetic variations of periods less than one day have been made to examine lateral inhomogeneities of crust and upper mantle electrical conductivity on a local scale (RIKITAKE, 1971).

Interpretation of observed geomagnetic variation anomalies has many problems; a major one being that the physical parameters of the source field which induces current flow in the earth are generally not well known. This makes it difficult to distinguish between geomagnetic variation patterns associated with the scale-length of the source field, and those associated with lateral changes of electrical conductivity within the earth. This problem has been partly overcome by the use of an array of simultaneously recording magnetometers placed in a grid over the survey area.

The 'coast effect' type of anomaly, characterised by large anomalous vertical variations near the ocean edge correlated with the component of horizontal variation perpendicular to the coast line, poses the additional major problem of the difficulty of distinguishing, on the basis of magnetic observations made only on the landward side of the coast line, between the effect of currents induced in the highly conductive sea water and the effect of current induced by a possible lateral change of conductivity structure beneath ocean and land (SCHMUCKER, 1970). Recent observations of telluric currents and magnetic variations made on the seaward side of the coast line suggest that such differences in conductivity beneath ocean and land do indeed exist (COX *et al.*, 1970; RICHARDS, 1970).

In early 1971 the authors conducted a study of magnetic variations across Southeast Australia, recording at 26 stations. Simultaneous records of the daily variation on three consecutive days of low storm activity were obtained at 24 of these stations. This paper presents an analysis of the data made at the periods of the first four diurnal harmonics. These variations, ranging from 6 to 24 hours in period, will penetrate the conductive oceans more easily than the higher frequency polar substorms and bays usually analysed in such studies, and may thus provide a more direct picture of suboceanic conductivity structure. The results of an analysis of substorms and bays, of periods less than three hours, recorded over the array have been presented elsewhere (LILLEY and BENNETT, 1972), and reference will be made to that paper as Paper 1 to avoid unnecessary duplication.

Magnetometer arrays are particularly useful in the separation of 'anomalous' vertical variations (such as those observed near ocean edges) from the large regional vertical variations, typical of the 'normal' field at diurnal periods. The essence of this separation lies in the scale-length of the array being greater than the typical scale-length of anomalous responses. It is important to be able to carry out this separation, because anomalous variations can affect the total vertical variation in both amplitude and phase in a quite complex way, as will be demonstrated.

An additional complexity is that the large 'normal' radial component of daily variation induces currents in the ocean on a global scale, (BULLARD and PARKER, 1970). These currents produce anomalies in the vertical components of the diurnal and its harmonics near the ocean edge, which are similar in character to the horizontally induced 'coast effect' anomalies mentioned above. The effect of induction in the ocean by vertical variations will be considered in a semi-quantitative manner in this paper, and its possible characteristics will be compared to the observed diurnal anomalies near the ocean edge.

The parameters of amplitude and phase will be used to describe variation fields of a particular frequency: phase will be particularly important, and the convention taken for its sign is now described.

For a time function which can be expressed

$$f(t)=A\cos\omega(t-t_g)$$

the phase t_g is a phase lag, (and it can, of course, be negative or positive. Negative phases may be made positive by adding to them integral values of the period, $2\pi/\omega$). If the function is expressed

$$f(t)=A\cos\omega(t+t_d)$$

then the phase t_d is a phase lead, and, of course,

$$t_d=-t_g\,.$$

If the time zero of a function is changed by δt to an earlier time, then the new phase lags and leads are given by

$$t'_g=t_g+\delta t$$
$$t'_d=t_d-\delta t\,.$$

If, for example, the function is determined relative to 14.00 GMT, and it is wanted relative to 00.00 GMT, then, for phases in hours,

$$t'_g=t_g+14$$
$$t'_d=t_d-14\,.$$

This paper will refer to other papers, some of which take phases as phase leads, and some as phase lags.

SCHMUCKER (1970) gives phase lags, as is shown by the increase of his diurnal phase values westward, (Schmucker's Tables 11–15), corresponding to the westward movement of the sun relative to the earth. By contrast, certain phases below will be calculated by taking the arctangent of the ratio (imaginary part/real part) of the Bullard-Parker-Richards stream function ϕ.

Now Bullard and Parker define the time variation of ϕ as

$$\phi=\phi_1 e^{i\omega t}\,,$$

where ϕ_1 is complex, say

$$\phi_1 = \phi_{1r} + i\phi_{1i} ;$$

then

$$\begin{aligned}\phi &= (\phi_{1r} + i\phi_{1i})e^{i\omega t} \\ &= Ke^{i\phi}e^{i\omega t} \qquad \text{for} \quad \frac{\phi_{1r}}{K} = \cos\phi , \quad \frac{\phi_{1i}}{K} = \sin\phi \\ &= K\left\{\cos\omega\left(t + \frac{\phi}{\omega}\right) + i\sin\omega\left(t + \frac{\phi}{\omega}\right)\right\} .\end{aligned}$$

Here it is understood that the real part of the right-hand side represents the actual time variation, thus by the convention just given above the phase ϕ/ω calculated from

$$\tan\phi = \frac{\phi_{1i}}{\phi_{1r}} ,$$

is a phase lead, (bearing in mind the respective signs of ϕ_{1i} and ϕ_{1r}, to obtain the correct quadrant for ϕ).

Except where otherwise specified, phases given in this paper are phase lags, and they are relative to 00.00 GMT.

2. Experimental Procedure

Twenty-five variometers were operated simultaneously at the sites shown in Fig. 1. Records from a twenty-sixth station, the permanent observatory of Toolangi (TLG), are published by permission of the Director of the Australian Bureau of Mineral Resources. Full details of operating procedure and recording interval are given in Paper 1 (LILLEY and BENNET, 1972).

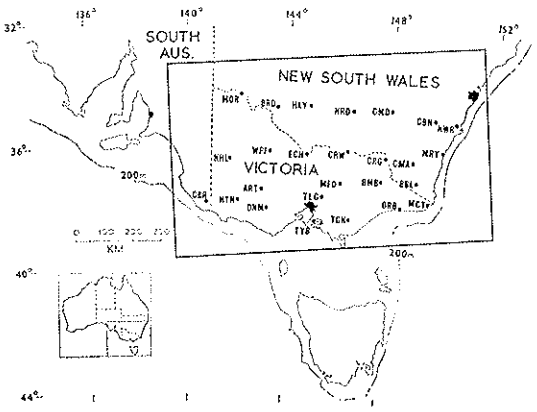

Fig. 1. Map of observing sites. The rectangle forms the frame for the contour maps of Figs. 4 to 7.

3. Data Reduction and Analysis

3.1 The data

Simultaneous records were obtained for 63 hours data, starting at 21.00 GMT on 23rd April 1971 and covering the three international quiet days of 24th–26th April, from 24 stations of the array. No records were obtained from HTN and TGN, and the record from BMB is incomplete. Drift of the traces occurred at ART due to the accidental uncovering of the instrument at that site during the second day.

3.2 Data reduction

Digitisation was performed manually by scaling the record films on a film reader. This process was very time consuming, and the following test was performed before complete digitisation to obtain the optimal digitising interval. The traces of a test station (TYB) were digitised at quarter hour intervals over the chosen data interval. Fourier analyses were then performed on the values taken in turn at quarter, half and hourly intervals. The spectra produced for digitising intervals of a quarter- and a half-hour were practically identical, with well marked peaks for the first four diurnal harmonics, whilst the spectra for the one-hour interval showed rather lower amplitudes and more diffuse peaks at the higher frequencies, due to the aliasing effect of power at periods less than 1 hour. A digitising interval of a-half-hour was thus chosen for all records.

The error of individual measurements is estimated as $\pm 1\gamma$ (gamma). The drift at ART was linearly corrected, and some attempt was made to manually smooth 'noisy' traces at MFD and NWR. The variograms of the digitised data are shown in Fig. 2.

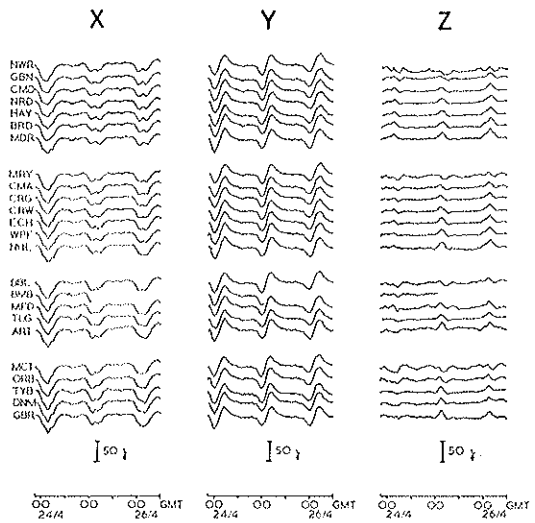

Fig. 2. Stacked variograms for the days 24–26 April 1971.

3.3 Data analysis

The frequency analyses were performed on the geographic components X (true north), Y (true east) and Z (downwards vertical) of the variations rather than the magnetic components H, D and Z recorded by the instruments. The use of geographic rather than magnetic components is quite acceptable in studies of the diurnal; for the mechanism producing the source field is such that spatial variations of the diurnal components are dependent on both geographic and geomagnetic coordinates (MATSUSHITA, 1967).

Frequency analysis proceeds in a similar manner to that in Paper 1. The data is represented in frequency components by the expression:

$$X_j = \tfrac{1}{2}A_0 + \sum_{K=1}^{n-1} \{A_K \cos(2\pi jK/2n) + B_K \sin(2\pi jK/2n)\} + \tfrac{1}{2}A_n(-1)^j \qquad (1)$$

where X_j, $j=0, \ldots, m-1$ are the digitised data points and $2n \equiv 2048$ is the length of data analysed after addition of zeros to the digitised data.

The Fourier coefficients,

$$A_K = \frac{2\Delta t}{T} \sum_{j=0}^{2n-1} X_j \cos(2\pi jK/2n)$$

are normalised by the digitised data length, thus

$$A_K' = \frac{T}{\tau} A_K \qquad (2)$$

where Δt is the digitising interval, $\tau = m\Delta t$ is the data interval, and $T = 2n\Delta t$. This normalisation enables direct comparison of these coefficients with those values in gammas obtained in global analyses of the diurnal, as defined by Matsushita's eq. 1. A point worth noting here is that since our data interval does not include the night hours of 26th April, when the daily variation is small, the addition of zeros to the data effectively creates a sample of three full days of diurnal variation, and normalisation by the digitised data length, 63 hours, gives values of the coefficients possibly 10% too large. Typical spectra are shown in Fig. 3.

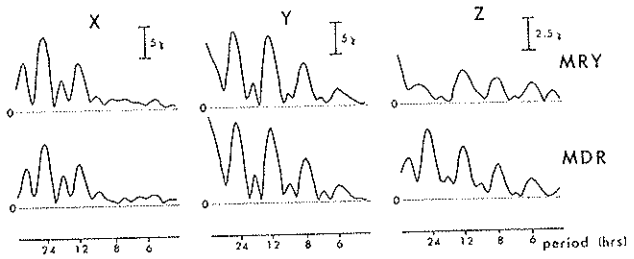

Fig. 3. Contrasting amplitude spectra for a 'normal' inland station, (MDR), and an 'anomalous' coastal station (MRY).

3.4 Errors of Fourier coefficients

The calibration constants of individual traces have a probable error of 2%. The errors in the Fourier coefficients due to digitising noise are calculated in the standard manner as in WHITTAKER and ROBINSON (1942) to be 0.1γ on the individual Fourier coefficients of Eq. 2. This gives a probable error for the 6-hour peak of the MRY Z spectrum of Fig. 3, for example, of order 10%. The accompanying phase error for this example is of order 0.05 hour.

4. Results

4.1 The contour maps

The amplitudes and phases of the Fourier coefficients at the diurnal frequency and its first three harmonics are plotted on base maps and contoured. Contour maps of components, X, Y and Z at periods 6, 8, 12 and 24 hours are

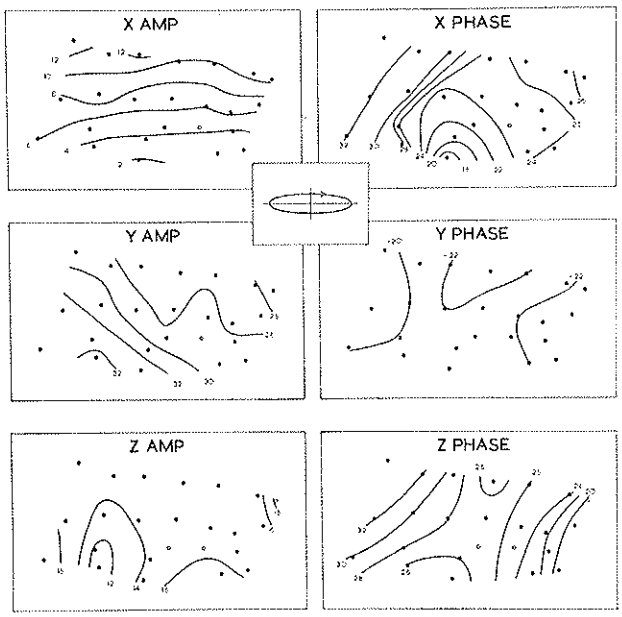

Fig. 4a. Contour maps of observed variations for 6-hour period. Units are 0.1 γ for amplitude, and 0.1 hr for phase.

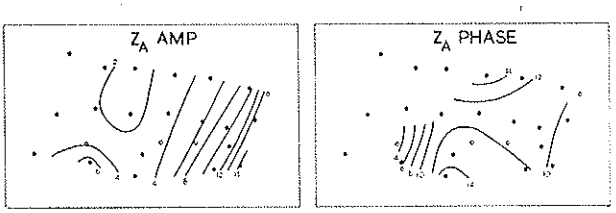

Fig. 4b. Observed vertical minus MDR vertical for 6-hour period.

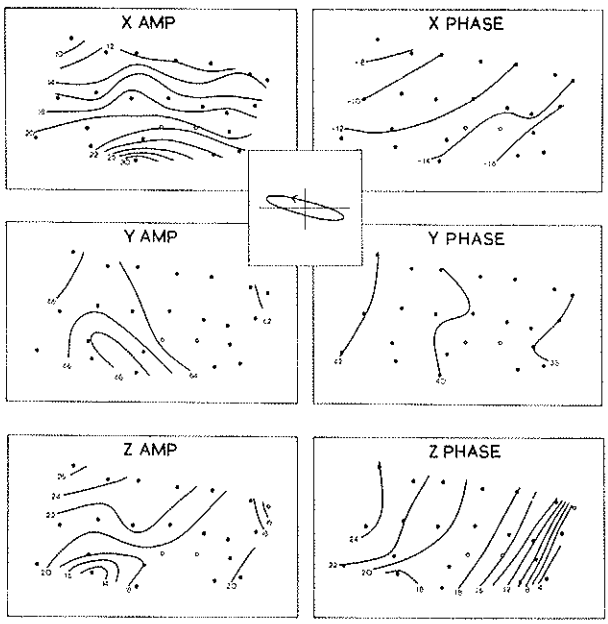

Fig. 5a. Contour maps of observed variations for 8-hour period. Units are 0.1 γ for amplitude and 0.1 hr for phase.

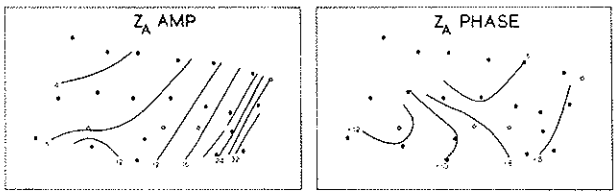

Fig. 5b. Observed vertical minus MDR vertical for 8-hour period.

presented in Figs. 4a, 5a, 6a and 7a, respectively. All phases are lags and are corrected to 00.00 GMT. The polarisation ellipses of the horizontal fields, as calculated for stations in the centre of the array by the method given in Paper 1, are included on the maps. Stations where records were incomplete or where individual components are considered unreliable are plotted as open circles (e.g., MFD Z).

4.2 Definitions of variation fields

Global magnetic potentials of the low harmonics of the diurnal have been calculated by several workers for different seasons and levels of solar activity (see MATSUSHITA, 1967). Such analyses assume that local anomalies of the internal portion of the variation field are of too small a spatial wavelength to systematically affect the variation over the global network of stations. Thus such potentials can only show changes due to either external variation field con-

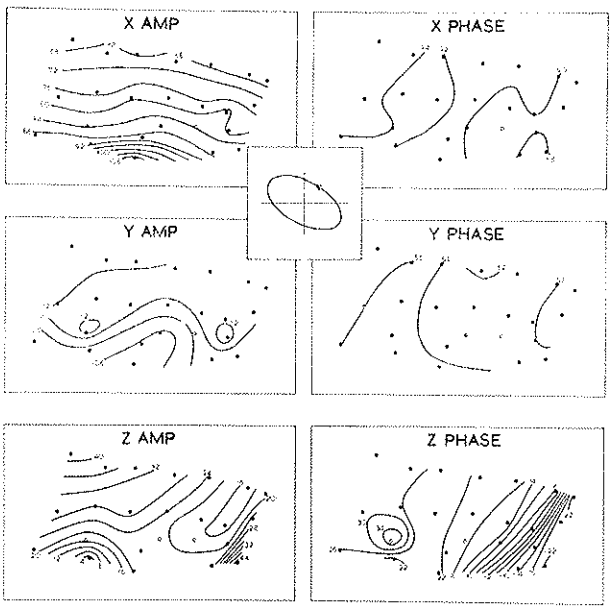

Fig. 6a. Contour maps of observed variations for 12-hour period. Units are 0.1 γ for amplitude and 0.1 hr for phase.

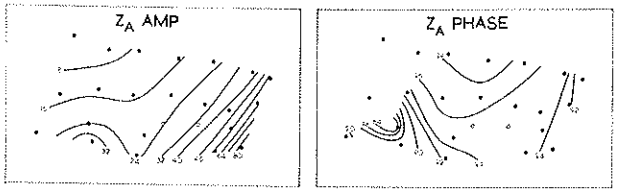

Fig. 6b. Observed vertical minus MDR vertical for 12-hour period.

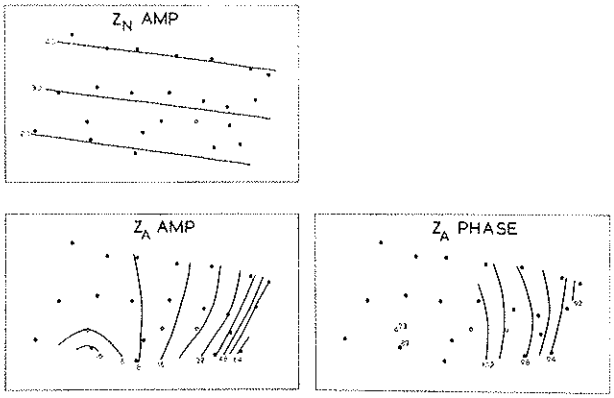

Fig. 6c. Normal field Z_N including gradient, and anomalous field Z_A formed by subtracting Z_N (using phase of MDR) from the maps of Fig. 6a.

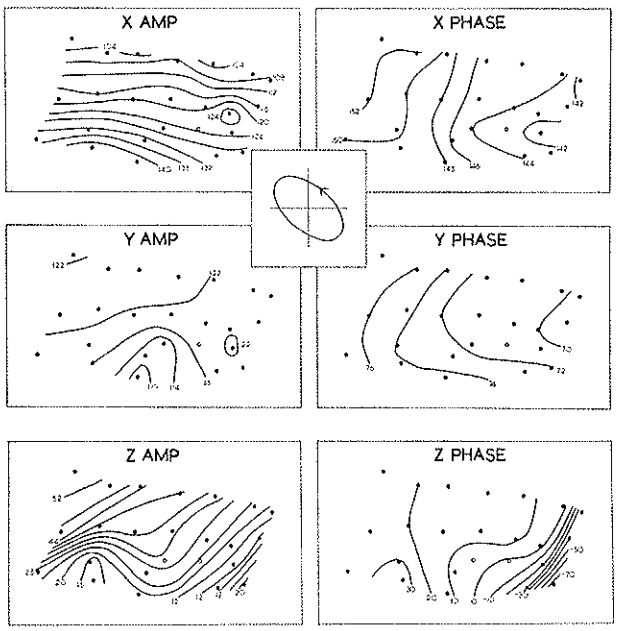

Fig. 7a. Contour maps of observed variations for 24-hour period. Units are 0.1 γ for amplitude and 0.1 hr for phase.

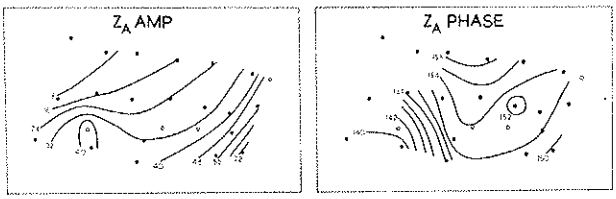

Fig. 7b. Observed vertical minus MDR vertical for 24-hour period.

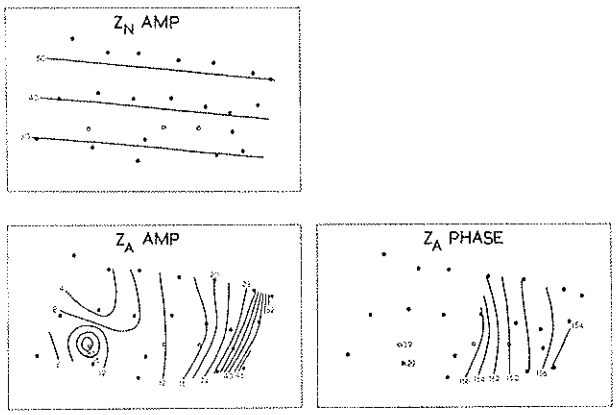

Fig. 7c. Normal field Z_N including gradient, and anomalous field Z_A formed by subtracting Z_N (using phase of MDR) from the maps of Fig. 7a.

figuration or non-radial conductivity changes in the earth of global scale lengths.

In this paper it is now assumed that the field $\boldsymbol{F}$ observed over the array is divisible into a 'normal' part, $\boldsymbol{F}_N$, which varies smoothly over the array, and 'anomalous' parts $\boldsymbol{F}_A^i$ which have spatial wavelengths of the order or less than the dimensions of the array. The 'normal' field, $\boldsymbol{F}_N$, is closely identifiable with that obtained from the global magnetic potentials, in as much as it varies on a global rather than local scale. The 'anomalous' fields $\boldsymbol{F}_A^i$ are assumed to be the result either of local (on the scale of the array) channelling of induced currents or distortion of the 'normal' induced current flow associated with local changes in lateral conductivity structure.

The observed magnetic variations $\boldsymbol{F}$ are therefore the vector sum:

$$\boldsymbol{F}(\boldsymbol{r}, t)=\boldsymbol{F}_N(\boldsymbol{r}, t)+\sum_i \boldsymbol{F}_A^i(\boldsymbol{r}, t)\,. \tag{3}$$

4.3 Discussion of results

Figures 4a, 5a, 6a and 7a show the basic contour maps for the first four harmonics of the daily variation. At all the frequencies a similar picture develops, described as follows.

The horizontal field components X and Y typically show a steady east-west increase of phase of from 0.2 to 0.8 hours across the array. This is identifiable with the westward movement of the daily variation over the earth's surface, which should produce approximately 40 minutes phase shift across the array. (The apparent complexity of the X phase in Fig. 4a may be due to the low amplitude and corresponding low signal/noise ratio of the X component at 6 hours, although even here the phase difference at the east and west extremes of the array is about 0.7 hour).

The amplitudes of the X and Y components vary smoothly across the array. The X component in particular shows an exceedingly smooth amplitude increase in the southwards direction. This is identifiable with the normal field variation due to the presence of the auroral electrojet to the south.

The vertical (Z) component shows more structure in both amplitude and phase, changes in both occurring predominantly in a northwest-southeast direction. The rate of change of phase of Z is largest on the eastern side of the array, with a total phase change across the array of nearly 180° at each frequency. The amplitude of Z typically falls from a large value in the northwest to a minimum trough in the centre or eastern part of the array, before rising again towards the southeast. This amplitude trough is best seen in the 12-hour Z component (Fig. 6a) and it is one of the most remarkable results of the present analysis.

The amplitude 'troughs' and the large phase shifts of the Z components can be considered as due to the vector addition of normal and anomalous vertical components, Z_N and Z_A, respectively, as in Eq. 3.

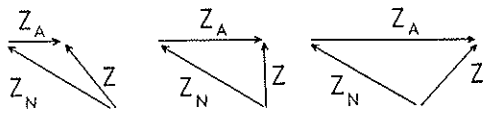

Fig. 8a. Typical vector composition of observed variations.

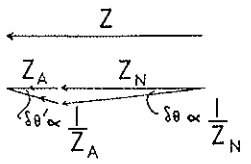

Fig. 8b. Large anomalous phase error ($\delta\theta'$) produced by subtraction of normal field (Z_N).

Figure 8a demonstrates schematically how a Z_A of given phase but varying amplitude can produce such anomalies of total variation, Z, in both amplitude and phase.

Smaller anomalies of both amplitude and phase are observed in the southwest corner of the array.

5. Separation of Normal and Anomalous Vertical Fields

5.1 *First step: removal of an estimated normal variation field*

The large anomalous changes of Z amplitude and phase in the east and southeast of the array are clearly associated with the ocean to continent lateral conductivity changes in the region of the Australian east coastline, whilst similarly the variations of Z in the southwest are also anomalous, being connected with the southern ocean and/or the possible conductivity anomaly near the recent volcanics of Victoria suggested in Paper 1.

The size of both above anomalous variations appears to be small in the northwest of the array, where both amplitude and phase of Z vary smoothly. Thus a first approximation to removal of a global type normal field, Z_N, is to subtract vectorially the Z response at a northwesterly station such as MDR. Figures 4b–7b show the first stage anomalous Z_A amplitude and phase maps resulting from the removal of Z_{MDR} from Z. For small anomalous Z_A vectors, e.g., at BRD and NHL, the subtraction of Z_{MDR} from Z will pass on into the resultant Z_A an error in phase of $\delta\theta'$ given by:

$$\delta\theta' \simeq \delta\theta \frac{Z_{MDR}}{Z_A} .$$

where $\delta\theta$ is the phase error compounded in the subtraction of Z_{MDR} from Z. Figure 8b shows diagrammatically this situation for near collinear Z, Z_N and Z_A vectors. For such stations no effort has been made to contour the Z_A phase maps.

The anomalous Z_A maps at all periods now show the amplitude decreasing rapidly away from the east coast, whilst the phase maps show much smaller variation than before. The southwest anomaly shows in both amplitude and phase, with phase decrease of up to 45° (1½ hours) at the 12-hour period, and 30° (2 hours) at the 24-hour period.

5.2 Second step: allowance for the spatial gradient of the normal variation field

Thus far, no allowance has been made for a possible smooth normal variation of Z_N across the array. As remarked above, the X component at all periods shows a smooth increase in amplitude in a southerly direction, due to the presence to the south of the eastwest flowing current concentrations in the auroral electrojet. Similarly the effect of the auroral electrojet on the normal variation will be a smooth decrease in amplitude of Z_N in a southerly direction.

Calculation of this change in Z_N at the 12 and 24-hour periods (only) is made by reference to Matsushita's Figs. 5a-c, and 6a-c, which show smoothed dip-latitudinal distributions of amplitude and phase of the variation components in different zones of the earth.

The observed normalised rates of southerly increase of X, $1/X \cdot \partial X/\partial x$, (and also of $1/Y \cdot \partial Y/\partial x$), correspond closely to those estimated from Matsushita's curves, (cf. Tables 1 and 2), and accordingly the normalised rate of southerly decrease of Z_N, $1/Z \cdot \partial Z/\partial x$ is taken as that estimated from Matsushita, (see Table 2). Estimation of the direction of decrease of Z_N in this region was guided by that suggested from the X contour maps of Figs. 6a and 7a.

It should be stressed that the amplitude variation of Z_N thus created is an approximate estimate made solely to separate out the anomalous fields, Z_A^i, more clearly, and does not necessarily reflect the average horizontally stratified conductivity beneath the array.

Second approximation anomalous amplitudes and phases are calculated as before by vectorial subtraction of Z_N from Z at every point and the resulting maps, together with the normal amplitude maps constructed by combining

Table 1. Observed values, phases lags relative to local midnight, for magnetic dip latitude 48°S. The values for Z are those observed at the inland station MDR.

Period (hr)	H		D		Z		$\frac{1}{X}\frac{\partial X}{\partial \theta}$	$\frac{1}{Y}\frac{\partial Y}{\partial \theta}$
	Amp (γ)	Phase (deg)	Amp (γ)	Phase (deg)	Amp (γ)	Phase (deg)	(deg. dip. lat.)$^{-1}$	(deg. dip. lat.)$^{-1}$
24	10.8	−10	12.7	242	5.2	175	0.07	$< -.01$
12	6.7	190	11.5	90	4.2	11	0.07	$< -.01$

Table 2. Values from Figs. 5 and 6 of MATSUSHITA (1967) for magnetic dip latitude 48°S. Phases lags relative to local midnight, (14.00 GMT).

Period (hr)	H		D		Z		$\frac{1}{H}\frac{\partial H}{\partial \theta}$	$\frac{1}{D}\frac{\partial D}{\partial \theta}$	$\frac{1}{Z}\frac{\partial Z}{\partial \theta}$
	Amp (γ)	Phase (deg)	Amp (γ)	Phase (deg)	Amp (γ)	Phase (deg)	(deg.dip.lat.)$^{-1}$	(deg.dip.lat.)$^{-1}$	(deg.dip.lat.)$^{-1}$
24	10	30	20	275	10	205	0.08 to 0.12	0.01	0.06
12	6	220	17	70	5	40	0.08 to 0.12	0.01	0.10

Table 3. Values observed at MRY (150°E, 36°S) on the coastline approximately 40 km from the edge of the continental slope. Phases are lags relative to 00.00 GMT. Y' is the horizontal component perpendicular to the east coast.

Harmonic of diurnal	Period (hr)	North X (X_N)			East Y (Y_N)			Vertical observed (Z)			Normal vertical (Z_N)			Anomalous vertical (Z_A)			Onshore horizontal (Y')		
		Amp (γ)	Phase		Amp (γ)	Phase		Amp (γ)	Phase		Amp (γ)	Phase		Amp (γ)	Phase		Amp (γ)	Phase	
			(hr)	(deg)		(hr)	(deg)		(hr)	(deg)		(hr)	(deg)		(hr)	(deg)		(hr)	(deg)
1	24	12.0	14.3	−150	12.0	7.0	105	1.2	−3.7	−55	4.3	2.2	33	4.3	15.4	−130	8.9	18.0	−90
2	12	7.6	9.0	−90	11.0	5.2	156	2.5	−2.1	−62	3.3	2.8	84	5.6	−2.7	−81	11.5	10.8	−36
3	8	1.8	−1.6	−72	6.3	3.8	169	1.9	0.5	22	2.6	2.0	90	2.8	7.0	−50	6.4	7.8	−10
4	6	0.6	2.6	155	2.8	−2.3	−138	1.5	1.9	114	1.5	2.8	168	1.5	1.0	60	2.5	1.0	60

Matsushita's spatial gradient with the MDR amplitude, are shown for 12 and 24 hours in Figs. 6c and 7c, respectively. The anomalous amplitude contours in the east are now aligned closely parallel to the east coast line. On the initial assumption of Section 5.1 that a coast effect is present, this is a good check on the reasonableness of the constructed normal amplitudes. The anomalous phase maps show a small westward phase increase, probably because no estimate of normal field phase variation was made, although it might be supposed that such phase variation should be similar to that of the X and Y components. Once again no attempt to contour the anomalous phase is made where the anomalous amplitude is small.

The approximate amplitudes and phases of all normal and anomalous components are listed in Table 3 for the station MRY, (150°E, 36°S). This site is on the coastline about 40 km from the edge of the continental slope. The spatial gradient correction has not been made for the 8- and 6-hour period data. Note that the phase values in Table 3 do not depend strongly upon Matsushita's global analysis. They do depend upon the assumption that the inland station MDR records a representative 'normal' field for this region. MDR and MRY lie on approximately the same geomagnetic dip latitude. Thus no appreciable difference in phase or amplitude of Z_A results from subtraction of Z_{MDR} from Z_{MRY} as compared to subtraction of Z_{MDR} with a spatial gradient correction applied in a dip longitudinal direction. The spatial gradient correction actually applied in Section 5.2 produces only small differences of Z_A phase compared to those obtained by the method of Section 5.1 (cf. Figs. 6b and 6c, Figs. 7b and 7c), although the Z_A amplitudes show somewhat larger differences between the two approaches.

6. Comparison of Observation with the Bullard-Parker-Richards Theory

6.1 The ocean induction model

Bullard and Parker have presented a theory of induction of electric currents in the oceans by the vertical component of the daily variation field. They present a global contour map of induced current flow in the oceans at the 24-hour period, and similar contour maps for 24, 12 and 8 hours are presented by Richards. Whilst BULLARD and PARKER (1970) and also RICHARDS (1970) estimate that their computational methods are satisfactory for periods greater than 6 hours, it should be noted that recently certain reservations have been made on this matter (E.C. BULLARD, B.A. HOBBS, personal communications, 1972). The conclusions drawn by comparing the present observations with Richards' calculations for 8- and 12-hour periods obviously depend upon this point.

Such computations take as inducing field the external daily variation as calculated from the global potentials of variation previously mentioned, over an earth uniformly underlain at a depth of order hundreds of kilometres by an

infinitely conducting mantle, to represent the radially symmetric increase in conductivity with depth suggested by Banks. The global contour maps obtained show the distribution of a magnetic stream function ϕ in the oceans; the actual oceanic current flow being given by:

$$\boldsymbol{j} = -\boldsymbol{n} \times \nabla_s \phi \qquad \text{where } \boldsymbol{n} \text{ is the outwards normal .}$$

The current flow is therefore clockwise around a minimum of ϕ.

Off the Australian east coast, the flow appears to be typically of uniform current density parallel to the coast (Bullard and Parker, Fig. 10). Thus an order of magnitude estimate of the anomalous vertical field due to the edge effect of these oceanic induction currents can be obtained from a model of infinitely extended lines of current in a semi-infinite thin conducting sheet (the sea water) flowing parallel to the edge of the sheet as shown in Fig. 9. The sheet is underlain by a perfect conductor at depth D. Then the vertical magnetic field B_z produced at 0, in the plane of the sheet, by surface current density j flowing from $y = -\infty$ to $+\infty$ in the sheet to a distance l from its edge is given by,

$$B_z = \frac{\mu_0}{2\pi}\int_a^{a+l} \frac{j\,dx}{x} + \text{effect of image currents in the mantle}$$

$$= \frac{\mu_0 j}{2\pi}\left\{\int_a^{a+l}\frac{dx}{x} - \int_a^{a+l}\frac{x\,dx}{x^2+4D^2}\right\}$$

$$= \frac{\mu_0 j}{2\pi}\cdot\frac{1}{2}\log_e\left\{\frac{(a+l)^2(a^2+4D^2)}{a^2[(a+l)^2+4D^2]}\right\} \tag{4}$$

$$\simeq \frac{\mu_0 j}{2\pi}\left\{\log_e\left[\frac{2lD}{(l^2+4D^2)^{1/2}}\right] - \log_e a\right\} \quad \text{for} \quad a \ll l \quad \text{and} \quad a \ll D\,. \tag{5}$$

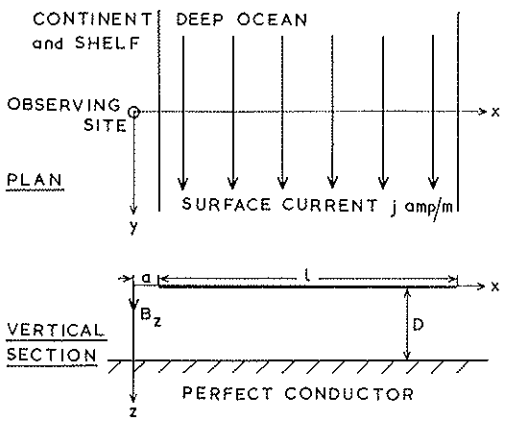

Fig. 9. Model of infinitely extended lines of current for the approximate calculation of Bullard and Parker's ocean induction effect.

6.2 Choice of parameters

The distance a is taken as 40 km for comparison of the results with those of Table 3.

The depth D is given on the individual ϕ contour maps. The equivalent surface current density j is estimated from the contour density of ϕ. In the case of Figs. 9 and 10 of Bullard and Parker, $j \simeq 3.2 \times 10^{-3}$ amp/metre for ϕ in quadrature, and $\lesssim -0.4 \times 10^{-3}$ amp/metre for ϕ in phase. Equation 4 is fairly insensitive to choice of l for large values of l, for example the value of B_z for $l = 5000$ is only 30% larger than that for $l = 500$ km. Choice of l is therefore made from an estimate of the distance to which the current flow is roughly parallel to the Australian east coast on the ϕ contour maps.

The source field in Bullard and Parker's Figs. 9 and 10 is that derived by Benkova for the northern summer of a year of low solar activity. Richards uses the source field derived by Hasegawa and Ota, which is a yearly average for a quiet year and is more appropriate to the southern hemisphere autumn. The magnitude of the source field is dependent on solar activity, and corrections to the values in Richards' contour maps are made by reference to Matsushita's Fig. 17, (the relative sun spot number of April 1971 was 70).

The results of the order of magnitude estimate are summarised in Table 4 for periods of 8, 12 and 24 hours.

6.3 Comparison of ocean induction model with observations

The ocean induction estimates of anomalous vertical field in Table 4 show marked differences to those of the observed anomalies in Table 3. These may reflect the inadequacies of the global potentials used in deriving the ocean induction effect. The present observations demonstrate how vertical daily variations several hundred kilometres inland may show some anomalous 'coast effect.' Since so many permanent magnetic observatories are situated near ocean edges, systematic errors in the calculated global magnetic potentials may have occurred. In the following comparison in terms of the parameters of amplitude and phase, no such errors in the global magnetic potential are allowed for.

6.4 The amplitudes

The amplitudes of the ocean induction calculations are rather smaller than the observed anomalies, particularly at the higher harmonics. The difference appears significant even within the limitations of the plane surface model used (Fig. 9). Several possible causes of error are now considered.

(1) It is possible that the quiet days analysed are not typical of those represented by the global potentials used as sources for the ocean induction effect. Comparison with Matsushita shows that the second and third day's data are typical quiet day variations for this region and season. The first day's data

Table 4. Values calculated from the maps of RICHARDS (1970) for the Bullard-Parker effect at station MRY (150°E, 36°S). Electric currents flowing in the ocean parallel to the east coast of Australia are taken as positive if they flow southwards. Phases are relative to 00.00 GMT. The values for B_Z are to be compared with the values for Z_A in Table 3.

Harmonic of diurnal	Period (hr)	Richards' figure	D (km)	l (km)	a (km)	Current density (amp/metre $\times 10^8$)		Phase lead of j $=\arctan(j_I/j_R)$ (deg)	Phase lag of j (deg)	Solar activity correction (% increase)	Vertical field B_Z	
						real j_R	imag. j_I				Amp (γ)	Phase lag (deg)
1	24	16	408	1000	40	−0.7	4.0	90 to 120	−90 to −120	30	3.0	−90 to −120
2	12	18	150	1000	40	0.7	2.5	−60 to −80	60 to 80	30	1.3	60 to 80
3	8	19	100	1000	40	0.7	2.0	110 to 130	−110 to −130	20	0.8	−110 to −130
1	24	17	250	1000	40	−0.8	3.0	90 to 120	−90 to −120	30	2.0	−90 to −120

shows an increase in X and decrease in Z suggesting some northward shift of the current system on this day. Comparison of the normal field amplitudes (Table 1) with those of Matsushita (Table 2) suggests they are representative for the season and solar activity level, although the phases differ by up to 40 degrees, and the H and Z amplitudes reflect the changing character of the daily variations mentioned above.

(2) The assumption of uniform current density in the Fig. 9 model from examination of the global ϕ contour maps would appear justified by the good comparison between Richards' own detailed ϕ maps off Peru and his global maps, (compare Richards' Figs. 16–19 with 20).

(3) The presence of the infinitely conducting 'mantle' beneath the ocean has the double effect of reducing the current flowing in the ocean and of providing an opposite component to the anomalous Z (see Eq. 4). Complete removal of this 'mantle,' whilst unjustified physically, would increase the anomalous Z by values ranging from 100% at 8 hours to 15% at 24 hours.

6.5 The phases

The phase lag of oceanic induction currents flowing south parallel to the Australian east coast is given approximately by the negative of the arctangent of the local ratio of quadrature to real current density, as obtained from the global maps of the stream function ϕ, and listed in Table 4. The downwards vertical anomalous magnetic field at the east coast will have phase approximating that of the near-shore induction currents.

Comparisons of the phases of the stream function ϕ in Table 4 with the observed phases of Z_A in Table 3 reveal that the observed phase lag in the 24-hour period is slightly less than predicted by the model, in 12-hour period is about 150° less than predicted, and at 8-hour period is about 70° greater than predicted. From inspection of the two 24-hour period models in Table 4 it appears that the depth to the infinitely conducting mantle has little effect on the phase.

6.6 Conclusions on the induction model

Within the limitations of the methods of calculation it appears that the observed coast anomaly at the Australian east coast can readily be approached in amplitude by the values predicted from the oceanic induction effect, only by allowing the depth to the good conducting level in the mantle below the ocean to become greater than that predicted by Banks and Parker. This would be in contradiction to the results of Cox *et al.*, and Richards, who find good conductors at shallow depths beneath the oceans.

The observed phase at 8 and 12 hours cannot be accounted for by the ocean induction model.

7. The Parkinson Vector in the Daily Variation

At the higher frequencies of magnetic bays and substorms a linear correlation has often been observed between the anomalous vertical variations near ocean edges and the component of horizontal variation perpendicular to the coastline. The presence of this relationship in array studies can be recognised in both amplitude and phase by reference to the polarization of the horizontal field, as shown by BENNETT and LILLEY (1972). The presence of a Parkinson vector relationship near coast lines has been interpreted by many workers by a lateral change in conductivity structure beneath ocean and land. There is no generally accepted model for this conductivity change, and indeed some workers such as EDWARDS *et al.* (1971) have suggested that Parkinson vectors have their origin solely in the oceanic induction by the normal vertical variation. LILLEY and BENNETT (1973) have demonstrated that, for the uniform field case, the existence of a Parkinson vector relationship implies that anomalous vertical variations are due either to induction by an appropriate horizontal variation component, or to a consistent correlation between primary (or normal) field components. In the latter case induction by the vertical component may indeed produce the anomalous variations.

It is unlikely that a consistent correlation of primary field components exists for all transient events. Thus the Parkinson vector relationship observed at periods less than about 2 hours near this coastline for all magnetic substorm events (see Paper 1) suggests induction by the horizontal component perpendicular to the coastline as a cause of anomalous vertical fiield.

For the four diurnal harmonics examined in the present paper, the amplitudes and phases of the onshore horizontal component, Y', in the region of 150°E 36°S are listed in Table 3. Comparison of the amplitudes of anomalous vertical Z_A and horizontal variation Y' shows that for all four harmonics the ratio of Z_A/Y' is about 0.5. The phase of Z_A is less than that of Y' by 30° to 45° except at the 6-hour period, where the phase difference is small; although here both Z_A and Y' amplitudes are small and have correspondingly larger errors.

An approximately constant (or slowly varying) relationship between the amplitudes and phases of Z_A and Y' would therefore appear to hold across this diurnal frequency range (1–4c/day). This correlation is similar in form to the aforementioned Parkinson vector relationship, observed across a frequency bandwidth of about 0.5–2c/hr in the substorm data: the substorm relationships gave typical Z_A/Y' amplitude ratios of about 0.6, and $(Y'-Z_A)$ phase differences of about 20–40° in the same region. Thus one consistent explanation of the diurnal anomalies is that they indicate an extension of the frequency range over which induction by the horizontal component Y' produces significant anomalous vertical variations near the coast. This would imply the existence of lateral con-

ductivity contrasts between ocean and land at this coast-line of large enough magnitude to be easily discernable in the diurnal variation and its harmonics.

Further examination of Table 3 reveals that a slightly less well-defined correlation between Z_A and Z_N amplitudes and phases also exists at all four diurnal harmonics; as should be expected since Z_N and Y' are strongly linked due to the spatially coherent daily variation ionospheric source currents. Thus induction by Z_N to give Z_A can still provide an alternative explanation. If this latter explanation is correct then Sections 6.3–6.6 have demonstrated, for the 8- and 12-hour harmonics at least, that such vertical induction must be of a substantially different form to that calculated by Richards.

8. Other Studies of Coastal Anomalies in the Daily Variation

In the light of the previous results it is of interest to reexamine other daily variation studies near ocean edges; to estimate the relative proportions of the effect of vertical induction in the oceans and the effect of induction by the horizontal component of the normal field perpendicular to the coast-line. Only studies made in geomagnetic mid latitudes will be considered here.

Some of the most valuable observations of daily variation are those of SCHMUCKER (1970) in western America. Estimated values of normal and anomalous components of a typical line CAB–BIS (SCHMUCKER, 1970, p. 157) together with the estimated anomalous vertical amplitude and phase calculated as before from Richards' figures, are shown in Table 5 for 8- and 12-hour periods; (Schmucker did not give observations for the 24-hour period, suspecting them of being in error). CAB is a coastal station and BIS an inland station where variations are considered representative of the regional normal field. Values for a of 50 km and for l of 1000 km are taken; and the values of j and D are again as given by Richards. The good conductor predicted at shallow depths below the ocean in this region by COX *et al.* (1970) would tend to dampen ocean induction currents and reduce the vertical induction anomalous amplitude below that estimated from Richards' figures.

Comparison of the observed and calculated values in Table 5 shows that the anomalous phases observed do not appear to match those expected from the vertical induction model, again indicating that this model does not adequately account for the ocean-edge effect: compare 176° against −60° for the 12-hour period, and 28° against −45° for 8-hour period. Instead, the amplitude ratio of observed anomalous vertical (Z_A) to onshore horizontal (Y') is about 0.5 to 0.6 at both 12- and 8-hour periods; whilst at both periods the phases of anomalous vertical near the ocean edge appear to be less by between 20° and 50° than those of the onshore horizontal. These results are strikingly similar to the values observed at the Australian east coast.

Table 5. Adapted from SCHMUCKER (1970) table 15 p. 157, and RICHARDS (1970) Figs. 18 and 19. Compare Z_A with B_Z, (use Phase 3). H, D and Z taken as for Schmucker's CAB, Z_N as for BIS. Y' is the onshore component at CAB, (declination of CAB is 16½°E).

Harmonic of diurnal c.p.d.	Period (hr)	From Schmucker's observations, (phase lags relative to 00.00 120° WMT)												From Richards' calculations			
		H		D		Z		Z_N		Z_A		Y'		B_Z			
		Amp (γ)	Phase (deg)	Amp (γ)	Phase (deg)	Amp (γ)	Phase (deg)	Amp (γ)	Phase (deg)	Amp (γ)	Phase (deg)	Amp (γ)	Phase (deg)	Amp (γ)	Phase 1 (deg)	Phase 2 (deg)	Phase 3 (deg)
2	12	6.7	187	9.3	274	7.5	193	3.6	213	4.3	176	7.7	225	1.2	180	180	−60
3	8	4.6	19	5.6	97	5.2	34	2.1	43	3.2	28	5.6	47	0.8	45	−45	−45

For B_Z, phase 1 is the phase lead of the ocean currents flowing northward parallel to the coast of California relative to 00.00 GMT; phase 2 is the phase lag corresponding to phase 1; phase 3 is the phase lag relative to Schmucker's time, (00.00 120° WMT = 08.00 GMT).

phase 3 = phase 2 − 120° × c.p.d.

The studies of RIDDIHOUGH (1969) in northwest Europe reveal a sizeable ($\sim 2\gamma$) anomaly in vertical daily variations near the Atlantic ocean edge. The Fig. 9 simplification does not seem appropriate here, but the low contour density of the stream function suggests small vertical induction anomalies. The same point also applies in reference to the total field results of SRIVASTAVA (1971) in eastern Canada. The changing anomalies in amplitude and phase along this curved coastline might suggest induction by the onshore horizontal component and could confirm the lateral conductivity contrasts in this region suggested by HYNDMAN and COCHRANE (1971).

9. Conclusions

An array experiment has enabled a thorough examination of the coast effect at the diurnal frequency and its low harmonics. Unlike shorter period variations, for which the normal vertical field is small, at periods of 24, 12, 8 and 6 hours there are substantial normal fields, which must be subtracted vectorially from the observed fields before the anomalous fields are studied.

Two main mechanisms may contribute to the large anomalous vertical fields observed in the first four diurnal harmonics at the Australian east coast. One explanation consistent with all observations is that these vertical anomalies are due in large part to induction by the onshore horizontal fields; implying lateral conductivity contrasts between ocean and land large enough to affect variations at these frequencies. Induction in the oceans by the vertical field, as described by Bullard and Parker, must also be considered; since order of magnitude estimates of this effect, based on the calculations of Richards, suggest that it should be observable. However, whilst such estimates for the basic diurnal harmonic may match the present observations, the parameter of phase discriminates strongly against a good match for the second and third harmonics. This mismatch is apparent both for eastern Australia and for the Californian Pacific region. The possible generation of magnetic variations by tidal movements of sea water has not been considered.

The smaller vertical anomaly observed in the southwest of the array is consistent with both the smaller ocean induction effect expected there and also the smaller onshore component of the horizontal field, as shown by the horizontal polarisation ellipses.

No anomalous variation has been separable in the horizontal fields although the small changes of the east (Y) component across the array may be anomalous. This result will be an important constraint for any theory seeking to explain the strong anomalous vertical variations.

An interpretation of this data in terms of electrical conductivity structure in the earth will be presented in a subsequent paper, which will also take into account the shorter period data from Paper 1. If the interpretation is now to

be in terms other than those of Bullard and Parker's vertical induction theory, the Bullard-Parker-Richards effect should in principle be taken into account, and subtracted before the anomalous fields are modelled.

The authors wish to thank Professor D.I. Gough who during the second half of his sabbatical visit to the Australian National University kindly lent them his array of magnetic variometers, and who has given much help and advice at all stages of the work.

One of the authors, (D.J.B.) was supported by a research scholarship awarded by the Australian National University.

REFERENCES

BANKS, R.J., Geomagnetic variations and the electrical conductivity of the upper mantle, *Geophys. J.R. astr. Soc.*, **17**, 457–487, 1969.

BENNETT, D.J. and F.E.M. LILLEY, Horizontal polarisation in array studies of anomalous geomagnetic variations, *Nature Physical Science*, **237**, 8–9, 1972.

BULLARD, E.C. and R.L. PARKER, Electromagnetic inductions in the oceans, in *The Sea*, edited by A.E. Maxwell, Vol. 4, pp. 695–730, Wiley-Interscience, New York, 1970.

COX, C.S., J.H. FILLOUX and J.C. LARSEN, Electromagnetic studies of ocean currents and electrical conductivity below the ocean-floor, in *The Sea*, edited by A.E. Maxwell, Vol. 4, pp. 637–693, Wiley-Interscience, New York, 1970.

EDWARDS, R.N., L.K. LAW and A. WHITE, Geomagnetic variations in the British Isles and their relation to electrical currents in the ocean and shallow seas, *Phil. Trans. Roy. Soc. London*, **A270**, 289–323, 1971.

HYNDMAN, R.D. and N.A. COCHRANE, Electrical conductivity structure by geomagnetic induction at the continental margin of Atlantic Canada, *Geophys. J.R. astr. Soc.*, **25**, 425–446, 1971.

LILLEY, F.E.M. and D.J. BENNETT, An array experiment with magnetic variometers near the coasts of south-east Australia, *Geophys. J.R. astr. Soc.*, **29**, 49–64, 1972.

LILLEY, F.E.M. and D.J. BENNETT, Linear relationships in geomagnetic variation studies, *Phys. Earth Plan. Interiors*, 1973, in press.

MATSUSHITA, S., Solar quiet and lunar daily variation fields, in *Physics of Geomagnetic Phenomena*, edited by S. Matsushita and W.H. Campbell, pp. 302–424, Academic Press Inc., New York, 1967.

PARKER, R.L., The inverse problem of electrical conductivity in the mantle, *Geophys. J.R. astr. Soc.* **22**, 121–138, 1970.

RICHARDS, M.L., A study of electrical conductivity in the earth near Peru, Ph.D. thesis, Univ. of California, San Diego, 1970.

RIDDIHOUGH, R.P., A geographical pattern of daily magnetic variation over North-West Europe, *Annales de Geophysique*, **25**, 739–745, 1969.

RIKITAKE, T., Electric conductivity anomaly in the earth's crust and mantle, *Earth-Sci. Rev.*, **7**, 35–65, 1971.

SCHMUCKER, U., Anomalies of geomagnetic variations in the southwestern United States, *Bull. Scripps. Inst. Oceanog.*, **13**, Univ. of California, 1970.

SRIVASTAVA, S.P., Diurnal variation of the total magnetic field along the east coast of Canada, *Earth Planet. Sci. Letters*, **10**, 423–429, 1971.

WHITTAKER, E.T. and G. ROBINSON, *The Calculus of Observations*, Blackie and Sons, London, 1942.